Turkish J. Eng. Env. Sci.
33 (2009) , 207 – 219.

doi:10.3906/muh-0906-41

Characterization of loose powder sintered porous titanium and Ti6Al4V alloy

Ziya ESEN[1], **Elif TARHAN BOR**[2], **Şakir BOR**[3]
[1]*Industrial Engineering Department, Çankaya University, 06530, Ankara-TURKEY*
e-mail: ziyaesen@cankaya.edu.tr
[2]*Central Laboratory, Middle East Technical University, 06531, Ankara-TURKEY*
[3]*Metallurgical and Materials Engineering Department, Middle East Technical University, 06531, Ankara-TURKEY*

Received 19.06.2009

Abstract

Porous titanium and Ti6Al4V alloy, biomedical candidate materials for use in orthopedic and dental implants, were manufactured by sintering the powders at various temperatures in loose condition. The characteristics of the corresponding powders and utilized sintering temperatures limited the final porosities in the range 30-37.5 vol. %. Similar to wrought alloys, compression stress-strain curves of porous samples exhibited 3 distinct deformation regions containing an elastic region, subsequent to yielding strain hardening region up to a peak stress and fast fracture after small straining. The mechanical properties of porous samples of both types were observed to obey minimum solid area (MSA) models in which the bond regions between particles perpendicular to loading direction are assumed to dominate in transmission of stress. A linear relation was obtained between yield strength and square of neck size ratio, $(X/D)^2$, where X and D represent the average neck and particle diameters, respectively.

Key Words: Porosity, Sintering, Titanium, Ti6Al4V Alloy, Mechanical Property

Introduction

Metallic materials used in biomedical applications, i.e. orthopedic prostheses, osteosynthesis devices, or dental implants, must possess mechanical properties similar to those of bone in addition to good corrosion resistance, bioadhesion, and biocompatibility (Barbucci, 2002).

Historically, stainless steel (X2CrNiMo1812, (316L)), CoCr-based alloys in the as-cast condition (CoCr30Mo6) or in the as-wrought condition (CoNi35Cr20), cp niobium, cp tantalum, cp titanium, and titanium alloys have been used as metallic biomaterials (Breme et al., 2003). Among them, the use of titanium and titanium alloys has become more frequent in recent times due to their high fatigue strength, low density in comparison to stainless steel and cobalt chromium alloys, and good 'in vivo' corrosion resistance due to the passive TiO_2 layer that forms in contact with air and other oxidizing elements in the body contacting the implant (Ricceri and Matteazzi, 2003).

However, the problem of stiffness related stress-shielding of bone has enhanced the search for low modulus materials especially in practical use of orthopedic prostheses. With regard to this, metallic foams are a new class of materials in biomedical applications due to their combined light weight and extremely low densities. Metallic foams to be used as biomaterials necessitate a low Young's modulus with sufficient compressive strength. Nevertheless, metallic foams may not exhibit sufficient compressive strength. Adjusting mechanical properties by applying appropriate heat treatment on metallic foams may be a good alternative for getting the required compressive strength values.

Differences in elastic moduli between natural bone and the implant materials may result in reduced tension/compression load or bending moment on the bone, which further causes bone mass loss and decreased bone thickness. This phenomenon is called 'stress shielding'. To reduce the elastic modulus, α/β titanium alloys having elastic modulus values approximately half those of the stainless steels or CoCr-based alloys have been introduced. However, the modulus of Ti6Al4V and related α/β alloys is still high (110 GPa) compared to human bone's (1-40 GPa). For minimizing the elastic moduli metastable β-titanium alloys such as Ti-13Nb-13Zr having elastic moduli ranging from 74 to 88 GPa have been presented. Among β-type alloys Ti-Nb-Zr-Ta has been used with moduli of 20%-25% lower than those of other available alloys (Long and Rack, 1998). However, there is still a mismatch in the mechanical properties of these materials and natural bone. In addition to these, reliable bone implant fixation is another problem. The use of surface textured or porous implants allows mechanical interlock of bone with the implant. Implant fixation by tissue ingrowth is further enhanced through the use of 3-dimensional open-pore structures allowing stresses to be transferred from the implant to the bone. Furthermore, it is possible to adjust the mechanical properties by close porosity control. That is to say, strength and elastic modulus values consistent with natural bone are possibly obtained in porous materials by alterations in porosity. To provide sufficient space for the attachment and proliferation of the new-bone tissues and the transport of the body fluids, the porous structure must possess high porosity.

For porous metals, 2 main types of production methods are liquid state and solid state processing (Banhart, 2001). Owing to the high melting temperature and chemical reactivity of titanium solid state foaming is a more promising method.

Porous titanium and titanium alloys can be produced using different solid state techniques, i.e. gas entrapment (Murray and Dunand, 2003), the space holder method either by using ammonium hydrogen carbonate (Wen et al., 2001; 2002) or by using a polymeric material as a spacer particle (Jee et al., 2000), and similar to the space holder method used in liquid processing technique for aluminum; using TiH_2 as foaming agent (Ricceri and Matteazzi, 2003), and finally conventional pressing and sintering (Oh et al., 2002). All these production methods yield porous titanium and titanium alloys with open porosities of 5-80 vol. %and pore size up to 500 μm. On the other hand, sintering hollow spheres of titanium (Karlsson et al., 2000) results in both an open and closed porous structure, which does not have widespread application as porous biomedical implant. Among these popular production techniques, loose powder sintering is a simple and economical one to get the required porosities ensuring the desired elastic modulus and strength values appropriate for biomedical applications.

In the present study, porous titanium and Ti6Al4V alloy were manufactured by sintering of powders at various temperatures in loose condition. Mechanical responses of porous samples were investigated under compression loading, which is predominant on materials implanted in the body, and the relation between mechanical properties (especially Young's modulus, E, and yield strength, σ_y, and total porosity content) were obtained. Eventually, the effect of bonding area, or neck size, between powder particles on yield strength of porous samples was also investigated.

Experimental

Materials

The starting materials were spherical titanium and Ti6Al4V alloy powders produced by PREP (Figures 1a and 1b). Both types of powders conformed to ASTM F 1580-01 specification designed for titanium and Ti6Al4V alloy powders for coating of surgical implants, and were supplied by Phelly Materials. As determined by using a Malvern Mastersizer 2000, titanium and Ti6Al4V alloy powders had bi-modal size distribution in the range 1-250 μm and monosize distribution in the range 45-250 μm with mean diameters of 74 μm and 107 μm, respectively (Figures 2a and 2b).

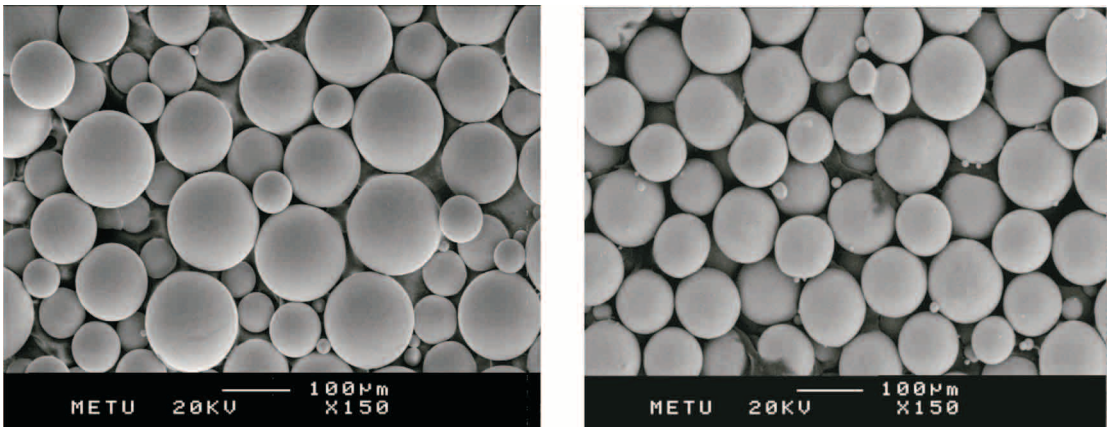

(a) (b)

Figure 1. SEM images of powders, (a) titanium, (b) Ti6Al4V alloy powders.

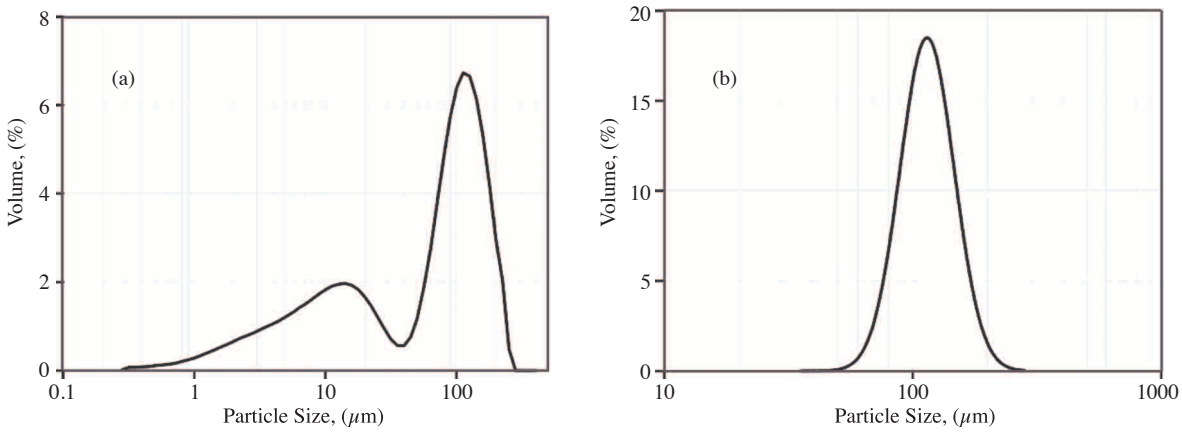

Figure 2. Particle size distribution curves for (a) titanium, (b) Ti6Al4V alloy powders.

Sintering and heat treatment

For loose powder sintering (sintering with no prior compaction), 30 mm long and 5.5 mm diameter cylindrical quartz crucibles were used to fill the powders under vibration. Absence of compaction eliminated the density variations caused due to die wall friction and also the deterioration of the powder due to the use of binders. Powders of both titanium and Ti6Al4V alloy were sintered for 1 h under high purity argon gas atmosphere.

While the titanium powders with an α/β transition temperature of 882 °C (Breme et al., 2003) were sintered at 850, 950, 1000, and 1050 °C, Ti6Al4V alloy powders with α/β transition temperature of 1000 ± 20 °C (Donachie, 1988) were sintered at 1000, 1050, 1100, 1150, 1200, and 1250 °C. The heating and cooling rates to/from corresponding sintering temperatures were around ∼50 °C/min and ∼20 °C/min, respectively. Prior to sintering, titanium sponge fines were placed at the top of the quartz crucibles to prevent excessive oxidation of powders throughout the sintering period. All sintering experiments were performed in a laboratory-type vertical tube furnace providing the possibility of rapid heating/cooling of samples to/from sintering temperatures.

Characterization

Total porosities of the sintered specimens were determined by Archimedes' principle,using highly volatile xylol ($CH_3C_6H_4CH_3$) with a density of 0.861 g/cm^{3}and a Sartorius precision balance (model CP2245-OCE) equipped with a density determination kit. Fractions of open and closed porosity were determined by weight measurements prior to and after dipping the samples in xylol for 36 h. Pore size distribution of titanium and Ti6Al4V alloy samples sintered at highest and lowest temperatures was determined using Quantachrome mercury porosimetry (0-50 psi, at 140°).

Microscopic analysis was performed by scanning electron microscopy (SEM) using a Jeol JSM 6400 Electron Microscope equipped with Noran System 6 X-ray microanalysis system. Cross-sections of epoxy-mounted sintered specimens were etched by Kroll's Reagent (3 mL HF + 6 mL HNO_3 + 100 mL H_2O). For each sample, at least 70 necks (interparticle bond) corresponding to particle size measurements were conducted on SEM micrographs.

For the compression tests carried out with a Shimadzu ACS-J 10 kN capacity universal tension-compression test machine at a cross-speed of 0.5 mm/min, sintered specimens were cut to 8.4 mm length by a diamond saw to obtain an H/D ratio of 1.5 and both surfaces of the specimens were mechanically ground to render them parallel. Teflon tape stuck on the die surfaces of the compression testing unit was employed to reduce the friction. Elastic moduli of the specimens were calculated from curves fitted to the linear elastic regions of the stress-strain curves, and the 0.2%-offset method was used to determine the yield strength.

Results and Discussion

Sintering of titanium and Ti6Al4V alloy powders

The change in porosity contents achieved by loose powder sintering of spherical titanium and Ti6Al4V powders with sintering temperatures is shown in Figure 3. One hour sintering of titanium and Ti6Al4V alloy powders under argon gas resulted in interconnected pores and porosities with average amounts systematically decreasing from 36.5% to about 30% with sintering temperature increasing from 850° to 1250 °C.

Upon sintering, the porosity of both pure titanium and Ti6Al4V alloy samples was observed to decrease linearly with increasing sintering temperature at almost the same rate as shown in Figure 3. Equations (1) and (2) represent the temperature (T) and dependencies of porosities (P) of titanium and Ti-6Al-4V alloy samples for the range studied, respectively;

$$P(\%) = 51.9 - 0.018 \times T(^{\circ}C) \quad R^2 = 0.9832 \tag{1}$$

$$P(\%) = 57.2 - 0.021 \times (T(^{\circ}C) \quad R^2 = 0.9810 \tag{2}$$

Higher porosities observed in Ti6Al4V alloy samples compared to the pure titanium ones in the same sintering temperature range can be attributed to the bi-modal distribution as well as the relatively smaller mean particle size of the latter. Since the compaction pressure is another factor, which changes the sintering response of powder particles in the same sintering temperature range, loose powder sintering with no compaction has been practiced in the present study to maximize the porosity content. A rather interesting feature observed in Figure 3 is that the porosity of the pure titanium sample sintered 850 °C, which is below the α/β transus temperature (882 °C), also obeys the general trend. It is well known that, due to the close packed structure, self diffusion coefficient of hcp-α titanium is orders of magnitude smaller than that of bcc-β titanium (Breme et al., 2003). Based on this fact, sintering is expected to be much slower below the β-transus temperature, yielding a smaller neck size (interparticle bond size) and higher porosity. The observed inconsistency may be elucidated by the dominance of surface diffusion over the bulk at early stages of sintering.

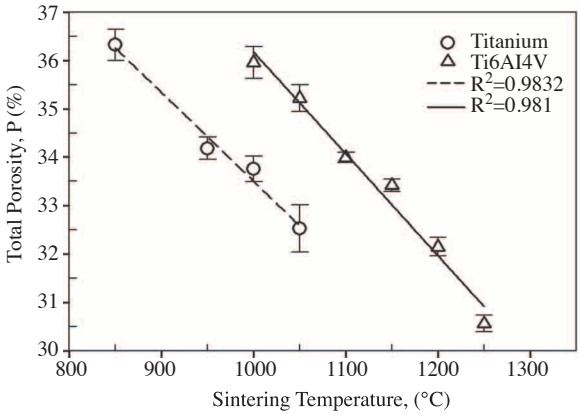

Figure 3. Temperature dependence of the total porosity content of sintered titanium and Ti6Al4V alloy powders.

Figure 4, which shows the polished cross-sections of the titanium and Ti6Al4V alloy powders sintered at 1000 °C, reveals irregular shaped interconnected pores. In loose powder sintering pore size and shape are dictated primarily by the powder size, shape and size distribution, and the sintering temperature and time. As can be seen in Figure 5, in both loose powder sintered titanium and Ti6Al4V alloy samples, although pore sizes up to 200 μm could be obtained occasionally, the average pore size was found to be around 30-40 μm and most of the pores were in the range 15 to 70 μm. Pore size distributions given in Figure 5 also reveal a slight shift of the pore sizes to smaller values with increasing sintering temperatures as expected.

In the solid state sintering the degree of sintering can be determined using density, porosity, or shrinkage measurements. Reduction in surface area also provides a gauge of the degree of sintering. However, in some cases, taking porosity or density as a single variable to determine the extent of sintering degree may be misleading since interparticle neck growth, with a loss of surface area, can occur without shrinkage depending on the sintering mechanism. Conversely, utilizing the change in average neck size ratio (X/D), where X and D represent the average neck and the powder particle diameters with sintering temperature, gives reliable and reproducible results about the sintering degree.

Figure 6 shows the change in average neck size ratio (X/D) with sintering temperature for titanium and Ti6Al4V powders sintered in loose condition. For titanium samples sintering temperatures between 850 and 1050 °C resulted in an average neck size ratio (X/D) between 0.142 and 0.277. On the other hand, average neck size ratios were found to be 0.177 and 0.312 for Ti6Al4V alloy powders sintered between 1000 and 1250°C.

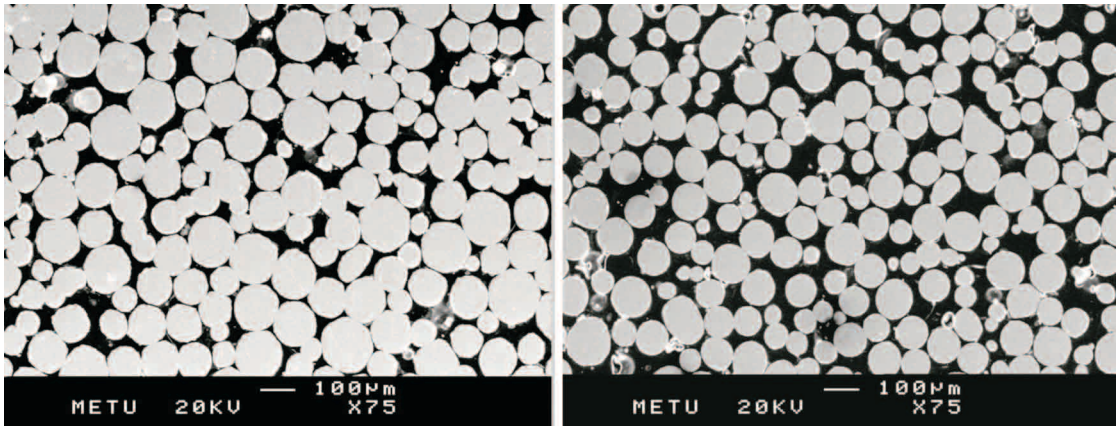

(a) (b)

Figure 4. Polished surfaces of samples sintered at 1000 °C; (a) titanium, (b) Ti6Al4V alloy.

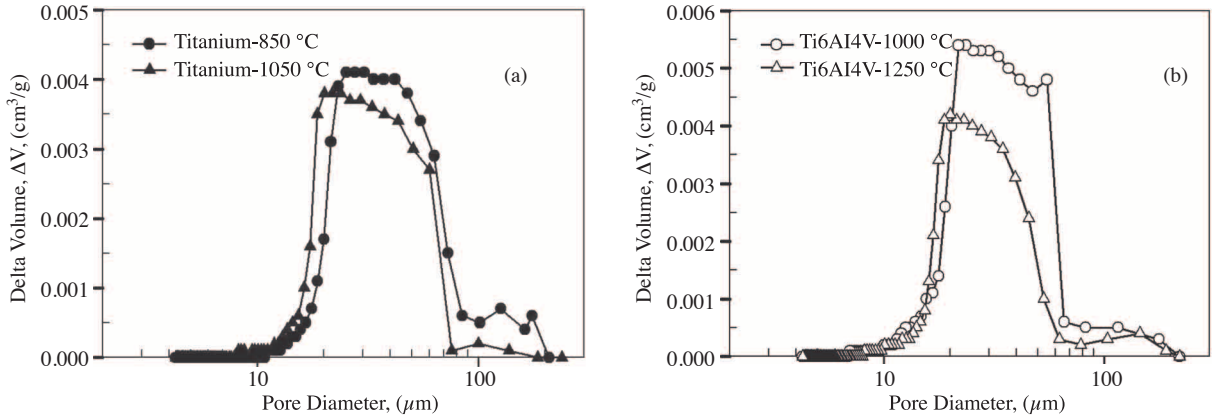

Figure 5. Pore size distribution in samples sintered at different temperatures; (a) titanium, (b)Ti6Al4V alloy.

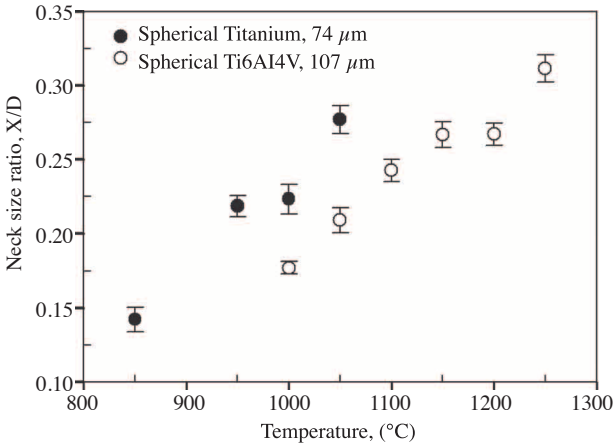

Figure 6. Neck size ratio change with sintering temperature.

In the loose powder sintering technique, as in all diffusion-controlled phenomena, temperature is the dominant factor affecting the sintering rate. Although the neck size is expected to change with sintering temperature in an exponential manner for constant soaking times, the relation obtained between average neck size ratio (X/D)

and sintering temperatures in the present study seems to be linear up to a temperature (Figure 6). However, sharp increases were detected in neck size ratio at sintering temperatures around 1050 and 1250 °C for loose powder sintered titanium and Ti6Al4V alloy powders, respectively. Dominance of a different type of transport mechanism may be the reason for such an occurrence. Further studies need to be carried out on this subject.

Microstructure

The mechanical property of a porous sample depends on its porosity content and the degree of sintering, and it is also largely affected by the underlying microstructure formed as a result of cooling from sintering temperatures or by applying a heat treatment subsequent to sintering. In addition to mechanical properties, microstructure can also change the properties of Ti6Al4V alloy in vivo and in vitro in biomedical applications. Although the surface roughness is held constant, small differences in the surface composition of various microstructures can modify the cell response (Lee et al., 2000). In Ti6Al4V alloy various microstructures were obtained by different heat treatment procedures. Possible phase morphologies can be either lamellar or equiaxed. In the present study, cooling of Ti6Al4V alloy samples at a rate of 20 °C/min under argon gas from sintering temperatures above the β-transus (1000 $\pm$ 20 °C) resulted in a lamellar type Widmanstätten structure (Figure 7). The dark regions, which are depleted from vanadium, correspond to the α-phase and the bright regions are the β-phase. The EDS spot analysis taken from some sintered compacts exhibited about 2.97 wt. % V and 6.58 wt. % Al in α-phase, and 6.84 wt. % V and 5.25 wt. % Al in β-phase.

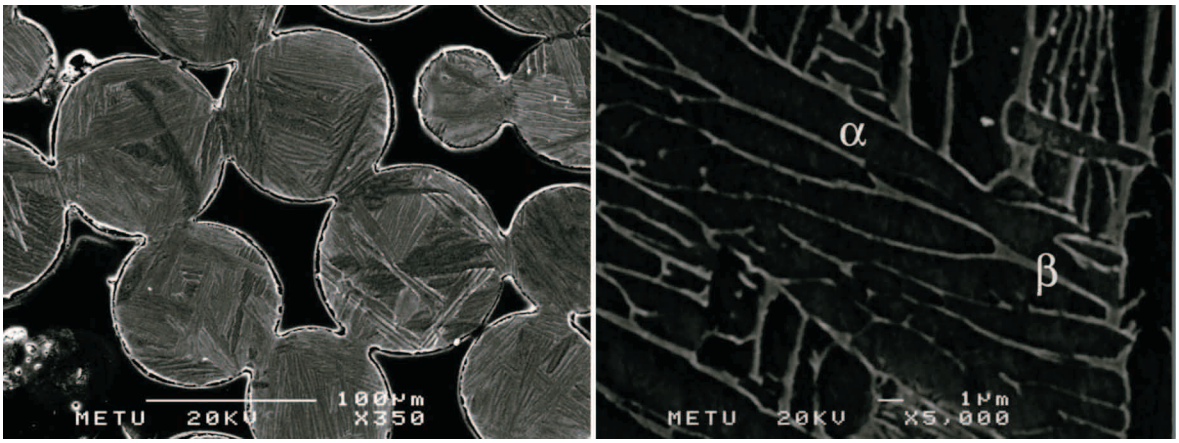

(a) (b)

Figure 7. SEM micrograph of porous Ti6Al4V alloy sintered at 1000 °C showing (a) sintering necks and Widmanstätten structure, (b) $\alpha - \beta$ colonies.

Stress-strain curves

Figure 8 shows the compression stress-strain curves of sintered powders. As it is expected and shown in the figure, mechanical properties of samples improved as their porosities decreased upon sintering at higher temperatures.

The curves of loose-sintered powders differ from those of highly porous titanium and Ti6Al4V alloy foams prepared by the space holder technique, which have compression stress-strain curves containing a linear elastic region, a long plateau stage with nearly constant flow stress to a large strain, and a densification stage, where

the flow stress increases sharply (Gibson and Ashby, 1999). A completely different mechanical response was observed in loose-sintered powders, i.e. almost linear elastic behavior at small strains, followed by yield and strain hardening up to an ultimate stress. Subsequent to a maximum or peak stress, fracture occurred after varying amounts of strain depending on the total porosity content. Internal damage such as voids or cracks in the neck region may cause softening of the material after the peak stress. These curves with an elastic region followed by a plastic region, ultimate stress, and fracture after small strain are rather similar to those of conventional wrought alloys.

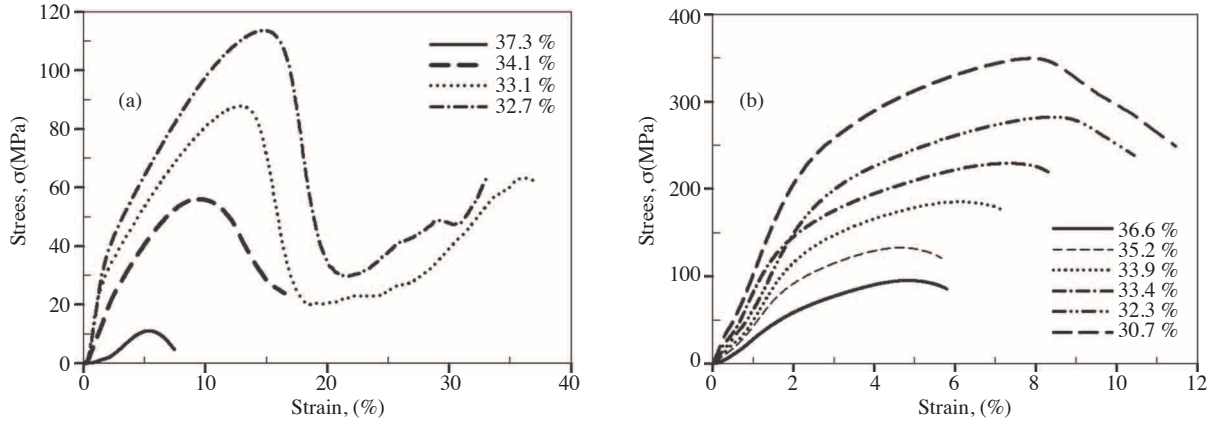

Figure 8. Compression stress-strain curves of samples having various amounts of porosities, (a) titanium, (b) Ti6Al4V alloy.

Porous samples failed with the formation of shear bands 45° to the compression axis by separation of contact zones (necks) between particles, as clearly seen in Figure 9a. Although surface cracks in the direction 45° to compression axis were observed as passing through the peak stress in some pure titanium samples, sintered at 1000 °C and 1050 °C, and having porosities 33.1% and 32.7%, respectively, samples did not fail until about 35% strain (Figure 8a). A microstructural investigation revealed that after fracturing of samples and tearing of bond regions, labeled with B in Figure 9b, bonded powders did not separate from each other completely. On the contrary, the contact area between powders increased over the neck region as the compression test proceeded, labeled with A in Figure 9b, and resulted in the formation of such a plateau region (Figure 8a).

Critical strain values at which shear banding starts at a peak stress were higher in titanium samples compared to Ti6Al4V alloy ones probably due to the ductile nature of titanium. For example, in the porous titanium sample sintered at 950 °C having an average neck size ratio (X/D) and porosity around 0.225 (Figure 6) and 34.1%, respectively, shear banding started at the 10% strain level (Figure 8a). On the other hand, for similar porosity level (33.9%) and similar average neck size ratio (0.235), the critical strain value was around 6% in the porous Ti6Al4V alloy sample sintered at 1100 °C (Figure 8b).

In addition, as can be seen from Figure 8b, critical strain values of sintered Ti6Al4V alloys with Widmanstätten microstructure were between 5% and 9%. It has been reported that in bulk Ti6Al4V alloys having similar Widmanstätten structures shear banding starts at 8%-10% strain (Silvia and Ramesh, 1997). Porous samples having relatively smaller critical strain values compared to bulk alloy in the present study might be originating from the coalescence of pores up to peak stress and due to sharp neck curvatures, which results in stress concentrations in the vicinity of neck curvatures.

In all samples ductile type of failure started by tearing of the necks as manifested by dimples in the fracture surfaces as clearly shown in Figure 10.

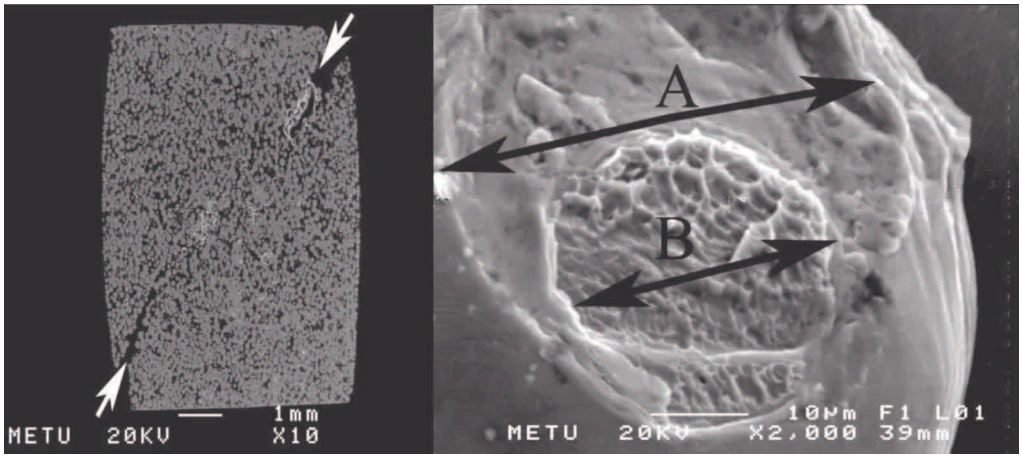

(a) (b)

Figure 9. Compression tested samples, (a) shear band formation in porous titanium, (b) fractured surface of porous titanium.

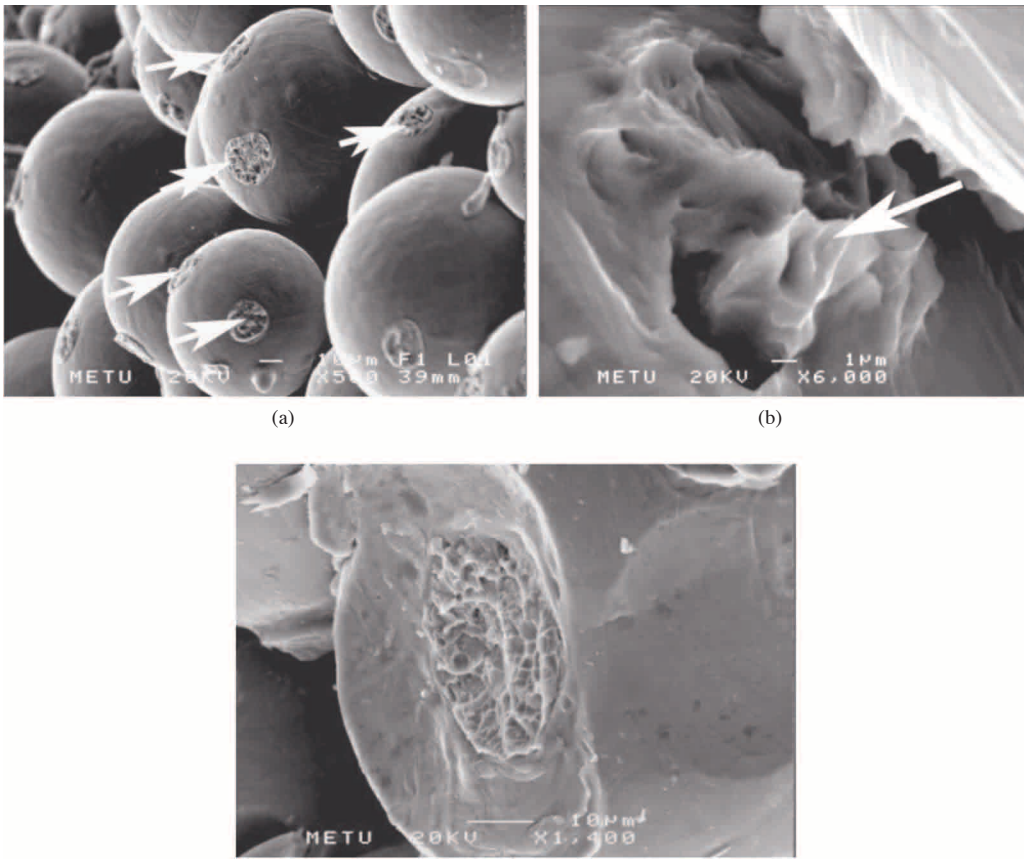

(a) (b)

(c)

Figure 10. SEM images of compression tested samples; (a) tearing of the necks in a Ti6Al4V alloy sample, (b) dimples in the fractured surface of titanium, (c) dimples in fractured surface of Ti6Al4V alloy.

Evaluation of mechanical properties

Young's moduli of both porous titanium (0.36-2.82 GPa) and Ti6Al4V alloy (3.9-11.4 GPa) samples produced in this study were close to that of human bone (1-40 Gpa) (Long and Rack, 1998) (Figure 11a). Moreover, titanium samples having porosities of 35.5-37.3 vol. % had yield strength values around 10.64-16.4 MPa, which is comparable to cancellous bone strength (0.6-16.3 MPa) (Dunham et al., 2005). Similarly, Ti6Al4V alloy samples with 34-35 vol. % porosity had yield strength values around 105-125 MPa, which is in the range of cortical bone's strength (104-121 MPa) (Bayraktar et al., 2004). In similar porosity ranges, porous Ti6Al4V alloy samples had considerably higher elastic modulus and yield strength values compared to pure titanium samples (Figure 11a and 11b), mainly due to inherent high mechanical properties.

It is essential to find out relations between mechanical properties and porosities of samples for close control of elastic modulus and yield strength in the final sintered product. To describe the dependence of the mechanical properties of materials on their porosities, numerous empirical and theoretical relations have been proposed. Within the porosity range of the present study, both Young's modulus (E) and yield strength (σ_y) were observed to vary linearly with increasing porosity (P) (Figures 11a and 11b) and to obey the following relations:;

$$E(GPa) = 24.1 - 0.64 \times P(\%) \tag{3}$$

$$\sigma_y(MPa) = 200.7 - 5.07 \times P(\%) \tag{4}$$

for pure titanium, and

$$E(GPa) = 52.5 - 1.32 \times P(\%) \tag{5}$$

$$\sigma_y(MPa) = 955.7 - 24.2 \times P(\%) \tag{6}$$

for Ti6Al4V alloy samples.

As seen in Figures 11a and 11b the property of interest decreases as the porosity content increases; then going to zero at a critical porosity, P_c, the percolation limit, is where the bond area between particles goes to zero. For powder materials, P_c is the tap porosity before sintering. The value of the critical porosity is a function of powder size, shape, their distribution, and the preparation method (Kováčik, 1999; 2001). Based on the following Figure 11, tap porosity for titanium powders is between 38% and 39%, whereas it changes between 39% and 40% for Ti6Al4V alloy powders.

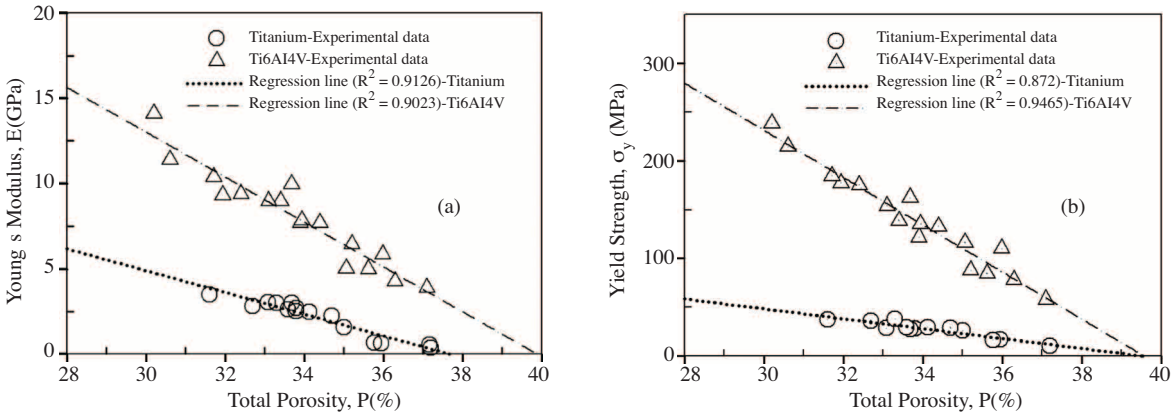

Figure 11. Mechanical property change with porosity, (a) Young's modulus, (b) yield strength.

Most porous bodies manufactured using powder metallurgical techniques contain more than one type of porosity, e.g. partially sintered bodies of various particle sizes and packing, resulting in a varying porosity character. In addition, the same amount of porosity may be obtained for different shaped powders, e.g. angular and spherical, by utilizing various manufacturing methods. However, the resultant mechanical properties may vary in the same porosity range due to differences in the size of sinter bonds formed between powders. That is to say, when a porous sample loaded deformation is localized on contacts or necks between the particles specimens with larger necks are expected to have higher strength values. Similarly, in minimum solid area (MSA) models used to define mechanical property change, the minimum, rather than the average, fractional solid area, e.g. ratio of bond area to the particle cross-sectional area, is used as the controlling factor (Rice, 1996). MSA normal to the stress (or conductive flux) is assumed to dominate the transmission of stress (i.e. strain, fracture toughness or energy, or strength) or conductive (thermal and electrical) fluxes through a body. Similar to MSA models, Nice and Shaffer (1972) predicted the sintered strength of porous materials by an empirical model yielding the relation;

$$\sigma = \sigma_o \times A \times (X/D)^2 \tag{7}$$

where X and D are average neck and particle size, respectively, A is an empirical constant, and σ_o is the wrought material strength. Equations (8) and (9) represent the change in yield strength values of manufactured porous titanium and Ti6Al4V alloy with square of neck size ratio, $(X/D)^2$, respectively.

$$\sigma_y = 580.03 \times (X/D)^2 \tag{8}$$

$$\sigma_y = 2333.3 \times (X/D)^2 \tag{9}$$

The difference in the slope of these curves (Figure 12) arises from the differences in packing characteristics of powders and inherent material properties. Xu et al. (2002) defined empirical constant A in Eq. (7) as containing solid fraction, effective number of bonds or necks, and stress concentration factor.

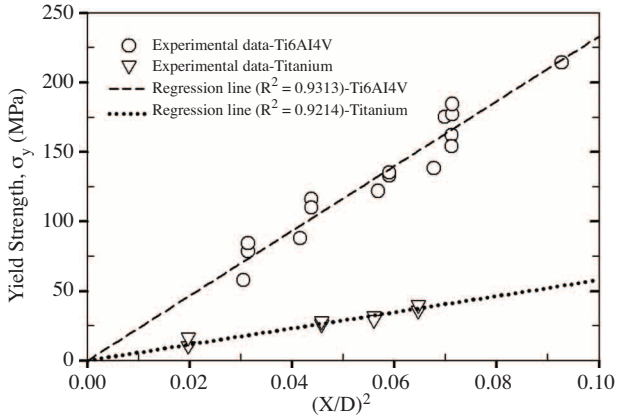

Figure 12. Yield strength change with square of neck size ratio, $(X/D)^2$.

Conclusions

Open porous titanium and Ti6Al4V alloy samples were produced by sintering of powders in loose condition. Porosity levels of titanium and Ti6Al4V alloy samples were 32.8–37.3 vol. % and 30–37.5 vol. % depending

on the sintering temperatures and characteristics of powders. Most of the pore sizes were found to be 15-70 μm with an average of around 30-40 μm. Higher levels of porosities may be achieved through loose powder sintering of monosized powders with higher average particle size.

Porous titanium and Ti6Al4V alloy samples had moduli of elasticity of 0.36-2.82 GPa and 3.9-11.4 GPa, respectively, and were observed to cover the range of human bones' modulus (1-40 GPa). Correspondingly, yield strengths of titanium samples (10.64-16.4 MPa) with porosities of 35.5-37.3 vol. % were around cancellous bone strength (0.6-16.3 MPa) (Dunham et al., 2005) and Ti6Al4V alloy samples with 34-35 vol. % porosity had yield strength values around 105-125 MPa comparable to those of cortical bone (104-121 MPa) (Bayraktar et al., 2004).

Stress-strain curves of manufactured porous titanium and Ti6Al4V alloys were similar to those of conventional wrought alloys and the plateau region present in stress-strain curves of metal foams was not observed. Highly porous metal foams fail by the formation of deformation bands perpendicular to the loading direction (Esen and Bor, 2007), whereas manufactured porous samples failed in a ductile manner by the formation of shear bands formed in the direction 45° to the compression axis.

Mechanical properties of sintered samples exhibited a linear dependence in the form $A \times (X/D)^2$, where A represents the proportional constant and $(X/D)^2$ is the square of neck size ratio.

Nomenclature

ASTM	American Society for Testing and Materials	MSA	minimum solid area
Bcc	body centered cubic	P_c	critical porosity
Cp	commercial purity	PREP	powder rotating electrode process
D	average particle diameter	SEM	scanning electron microscope
E	Young's modulus	X	average neck diameter
EDS	energy dispersive spectroscopy	α	alpha phase
H/D	height to diameter ratio	β	beta phase
Hcp	hexagonal close packed	σ_y	yield strength

Acknowledgments

This work has been supported by METU, Project # BAP-2005-03-08-05 and TÜBİTAK, Project # 104M121. The authors wish to thank METU Central Laboratory for particle and pore size distribution measurements.

References

Banhart, J., "Manufacture, Characterization and Application of Cellular Metals and Metal Foams", Progress in Materials Science, 46, 559-632, 2001.

Barbucci, R., Integrated Biomaterial Science, Kluwer Academic Publishers, Hingham, MA, USA, 2002.

Bayraktar, H., Morgan, E.F., Niebur, G.L., Morris, G.E., Wong, E.K. and Keaveny, T. M., "Comparison of the Elastic and Yield Properties of Human Femoral Trabecular and Cortical Bone Tissue", Journal of Biomechanics, 37, 27-35, 2004.

Breme, J., Eisenbarth, E. and Biehl, V., Titanium and Titanium Alloys, (ed. C. Leyens and M. Peters), Wiley-Vch, 2003.

Donachie, M.J. Jr., Titanium: A Technical Guide, Metals Park, ASM International, 1988.

Dunham, C.E., Takaki, S.E., Johnson, J.A. and Dunning, C.E., "Mechanical Properties of Cancellous Bone of the Distal Humerus", Clinical Biomechanics, 20, 834-838, 2005.

Esen, Z. and Bor, Ş., "Processing of Titanium Foams using Magnesium Spacer Particles", Scripta Materialia, 56, 341-344, 2007.

Gibson, L.J. and Ashby, M.F., Cellular Solids: Structure and Properties, 2^{nd} Edition, Cambridge University Press, Cambridge, 1999.

Jee, C.S.Y., Özgüven, N., Guo, Z.X. and Evans, J.R.G., "Preparation of High Porosity Metal Foams", Metallurgical Materials Transactions, 31B, 1345-1352, 2000.

Karlsson, K.H., Ylänen, H. and Aro, H., "Porous Bone Implants", Ceramic International, 26, 897-900, 2000.

Kováčik, J, "Correlation between Young's Modulus and Porosity in Porous Materials", Journal of Materials Science Letters, 18, 1007-1010, 1999.

Kováčik, J., "Correlation between Shear Modulus and Porosity in Porous Materials", Journal of Materials Science Letters, 20, 1953-1955, 2001.

Lee, T.M., Chang, E. and Yang, C.Y., "A Comparison of the Surface Characteristics and Ion Release of Ti6Al4V and Heat-Treated Ti6Al4V", Journal of Biomedical Materials Research, 50, 499-511, 2000.

Long, M. and Rack, H.J., "A Review: Titanium Alloys in Total Joint Replacement - A Materials Science Perspective", Biomaterials, 19, 1621-1639, 1998.

Murray, N.G.D. and Dunand D.C., "Microstructure Evolution during Solid-State Foaming of Titanium", Composite Science Technology, 63, 2311-2316, 2003.

Nyce, A.C. and Shaffer, W.M., "The Relationship of B.E.T. Surface Area to the Sintering Behavior of Spherical Copper Particles", International Journal of Powder Metallurgy, 8, 171-180, 1972.

Oh, I.H., Nomura, N. and Hanada, S., "Microstructures and Mechanical Properties of Porous Titanium Compacts Prepared by Powder Sintering", Materials Transactions, 43, 443-446, 2002.

Ricceri, R. and Matteazzi, P., "P/M Processing of Cellular Titanium", International Journal of Powder Metallurgy, 39, 53-61, 2003.

Rice, R.W., "Comparison of Physical Property-Porosity Behaviour with Minimum Solid Area Models", Journal of Materials Science, 31, 1509-1528, 1996.

Silva, M.G. and Ramesh, K.T., "The Rate-Dependent Deformation and Localization of Fully Dense and Porous Ti6Al4V", Materials Science and Engineering, A232, 11-22, 1997.

Xu, X., Lu Peizen and German, R.M., "Densification and Strength Evolution in Solid-State Sintering, Part II: Strength Model", Journal of Materials Science, 37, 117-126, 2002.

Wen, C.E., Mabuchi, M., Yamada, Y., Shimojima, K., Chino, Y. and Asahina, T., "Processing of Biocompatible Porous Ti and Mg", Scripta Materialia, 45, 1147-1153, 2001.

Wen, C.E., Yamada, Y., Chino, Y., Asahina, T. and Mabuchi, M., "Processing and Mechanical Properties of Autogenous Titanium Implant Materials", Journal of Materials Science: Materials in Medicine, 13, 397-401, 2002.